higher numbers from colon contents than was the nitrate respiration–deficient mutant (Fig. 3H and fig. S8B). Collectively, these data suggested that nitrate respiration conferred a marked growth advantage on commensal *E. coli* in the lumen of the inflamed gut.

The picture emerging from this study is that nitrate generated as a by-product of the host inflammatory response can be used by *E. coli*, and likely by other commensal Enterobacteriaceae, to edge out competing microbes that rely on fermentation to generate energy for growth. Obligate anaerobic microbes in the intestine compete for nutrients that are available for fermentation but cannot use nonfermentable nutrients (such as fermentation end products). The ability to degrade nonfermentable substrates probably enables *E. coli* to sidestep this competition, which explains the fitness advantage conferred by nitrate respiration in the inflamed gut. Through this mechanism, inflammation contributes to a bloom of nitrate-respiration–proficient Enterobacteriaceae, providing a plausible explanation for the dysbiosis associated with intestinal inflammation (*3–12*). This general principle might also influence the dynamics of host-associated bacterial communities outside the large bowel, as nitrate respiration confers a fitness advantage in the oxygen-poor and nitrate-rich environment of the cystic fibrosis airway (*21*).

References and Notes
1. P. B. Eckburg *et al.*, *Science* **308**, 1635 (2005).
2. R. E. Ley *et al.*, *Proc. Natl. Acad. Sci. U.S.A.* **102**, 11070 (2005).
3. A. Krook, B. Lindström, J. Kjellander, G. Järnerot, L. Bodin, *J. Clin. Pathol.* **34**, 645 (1981).
4. M. H. Giaffer, C. D. Holdsworth, B. I. Duerden, *J. Med. Microbiol.* **35**, 238 (1991).
5. P. Seksik *et al.*, *Gut* **52**, 237 (2003).
6. U. Gophna, K. Sommerfeld, S. Gophna, W. F. Doolittle, S. J. Veldhuyzen van Zanten, *J. Clin. Microbiol.* **44**, 4136 (2006).
7. D. N. Frank *et al.*, *Proc. Natl. Acad. Sci. U.S.A.* **104**, 13780 (2007).
8. M. M. Heimesaat *et al.*, *PLoS ONE* **2**, e662 (2007).
9. C. Lupp *et al.*, *Cell Host Microbe* **2**, 119 (2007).
10. B. Stecher *et al.*, *PLoS Biol.* **5**, e244 (2007).
11. M. Barman *et al.*, *Infect. Immun.* **76**, 907 (2008).
12. W. S. Garrett *et al.*, *Cell Host Microbe* **8**, 292 (2010).
13. J. O. N. Lundberg, J. M. Lundberg, K. Alving, P. M. Hellström, *Lancet* **344**, 1673 (1994).
14. I. I. Singer *et al.*, *Gastroenterology* **111**, 871 (1996).
15. A. Enocksson, J. Lundberg, E. Weitzberg, A. Norrby-Teglund, B. Svenungsson, *Clin. Diagn. Lab. Immunol.* **11**, 250 (2004).
16. C. Szabó, H. Ischiropoulos, R. Radi, *Nat. Rev. Drug Discov.* **6**, 662 (2007).
17. C. Schöneich, *Biochim. Biophys. Acta* **1703**, 111 (2005).
18. B. Balagam, D. E. Richardson, *Inorg. Chem.* **47**, 1173 (2008).
19. R. B. Gennis, V. Stewart, in Escherichia coli *and* Salmonella. *Cellular and Molecular Biology*, F. C. Neidhardt *et al.*, Eds. (ASM Press, Washington, DC, 1996), vol. 1, pp. 217–261.
20. M. C. Pils *et al.*, *Inflamm. Bowel Dis.* **17**, 2038 (2011).
21. L. R. Hoffman *et al.*, *PLoS Pathog.* **6**, e1000712 (2010).

Rif1 Prevents Resection of DNA Breaks and Promotes Immunoglobulin Class Switching

Michela Di Virgilio,[1] Elsa Callen,[3]* Arito Yamane,[4]* Wenzhu Zhang,[5]* Mila Jankovic,[1] Alexander D. Gitlin,[1] Niklas Feldhahn,[1] Wolfgang Resch,[4] Thiago Y. Oliveira,[1,6,7] Brian T. Chait,[5] André Nussenzweig,[3] Rafael Casellas,[4] Davide F. Robbiani,[1] Michel C. Nussenzweig[1,2]†

DNA double-strand breaks (DSBs) represent a threat to the genome because they can lead to the loss of genetic information and chromosome rearrangements. The DNA repair protein p53 binding protein 1 (53BP1) protects the genome by limiting nucleolytic processing of DSBs by a mechanism that requires its phosphorylation, but whether 53BP1 does so directly is not known. Here, we identify Rap1-interacting factor 1 (Rif1) as an ATM (ataxia-telangiectasia mutated) phosphorylation-dependent interactor of 53BP1 and show that absence of Rif1 results in 5′-3′ DNA-end resection in mice. Consistent with enhanced DNA resection, Rif1 deficiency impairs DNA repair in the G_1 and S phases of the cell cycle, interferes with class switch recombination in B lymphocytes, and leads to accumulation of chromosome DSBs.

The DNA damage response factor p53 binding protein 1 (53BP1) is a multidomain protein containing a chromatin-binding tudor domain, an oligomerization domain, tandem breast cancer 1 (BRCA1) C-terminal (BRCT) domains, and an N-terminal domain with 28 SQ/TQ potential phosphorylation sites for phosphatidylinositol 3-kinase–related kinases [PIKKs, ataxia-telangiectasia mutated (ATM)/ATM and Rad3-related/DNA-dependent protein kinase catalytic subunit (DNA-PKcs)] (*1–3*). 53BP1 contributes to DNA repair in several ways: This protein facilitates joining between intrachromosomal double-strand breaks (DSBs) at a distance (synapsis) (*4–7*), it enables heterochromatic DNA repair through relaxation of nucleosome compaction (*2, 3*), and it protects DNA ends from resection and thereby favors repair of DSBs that occur in G_1 phase by nonhomologous end joining (NHEJ) (*4, 5, 8*). Consistent with its role in DNA-end protection, 53BP1 is essential for class switch recombination (CSR) in B lymphocytes (*9, 10*).

Structure-function studies indicate that, besides the recruitment of 53BP1 to DNA ends, protection requires 53BP1 phosphorylation (*4*), but how this protective effect is mediated is unknown. To identify phosphorylation-dependent interactors of 53BP1, we applied stable isotope labeling by amino acids in cell culture (SILAC). *Trp53bp1*$^{-/-}$ (*Trp53bp1* encodes 53BP1) B cells were infected with retroviruses encoding a C-terminal deleted version of 53BP1 (53BP1^{DB}) or a phospho-mutant in which all 28 N-terminal potential PIKK phosphorylation sites were mutated to alanine (53BP1^{DB28A}) (*4*), in media containing isotopically heavy (53BP1^{DB}) or light (53BP1^{DB28A}) lysine and arginine (fig. S1, A to C) (*11*).

Most proteins coprecipitating with 53BP1^{DB} and 53BP1^{DB28A} displayed a $H/(H + L)$ ratio of ~0.5 (H, heavy; L, light), which is characteristic of phospho-independent association (average of 0.57 ± 0.09, peptide count: at least four) (Fig. 1 and table S1). Many of these proteins are nonspecific contaminants, but others such as KRAB-associated protein 1 (KAP-1), dynein light chain LC8-type 1 (Dynll1), Nijmegen breakage syndrome 1 (Nbs1), and H2AX represent authentic phospho-independent 53BP1-interacting proteins (fig. S1D). Three proteins displayed an abundance ratio that was more than four standard deviations (SDs) above the mean, indicating that these proteins interact specifically

[1]Laboratory of Molecular Immunology, The Rockefeller University, New York, NY 10065, USA. [2]Howard Hughes Medical Institute (HHMI), The Rockefeller University, New York, NY 10065, USA. [3]Laboratory of Genome Integrity and Center for Cancer Research, National Cancer Institute (NCI), National Institutes of Health (NIH), Bethesda, MD 20892, USA. [4]Genomics and Immunity and National Institute of Arthritis and Musculoskeletal and Skin Diseases (NIAMS), NCI, NIH, Bethesda, MD 20892, USA. [5]Laboratory of Mass Spectrometry and Gaseous Ion Chemistry, The Rockefeller University, New York, NY 10065, USA. [6]Department of Genetics, Faculty of Medicine, University of São Paulo, Ribeirão Preto, Brazil. [7]National Institute of Science and Technology for Stem Cells and Cell Therapy, Ribeirão Preto, Brazil.

*These authors contributed equally to this work.
†To whom correspondence should be addressed. E-mail: nussen@rockefeller.edu

with phosphorylated 53BP1: Pax interaction with transcription-activation domain protein-1 (Paxip1, or PTIP; 0.95), PTIP-associated protein 1 (Pa1; 0.97), and Rap1-interacting factor 1 (Rif1) (0.96) (Fig. 1 and figs. S1D and S2). PTIP was known to interact with 53BP1 in a phospho-dependent manner (12), whereas Pa1 and Rif1 were not.

Rif1 was originally identified in budding yeast as a protein with a key role in telomere length maintenance (13). However, in mammalian cells, Rif1 is not essential for telomere homeostasis, but has been assigned a number of different roles in maintaining genome stability, including participation in the DNA damage response (14–16), repair of S-phase DNA damage (17, 18), and regulation of origin firing during DNA replication (19, 20). However, the mechanism by which Rif1 might contribute to DNA repair and maintenance of genome stability is not known.

To confirm that Rif1 interaction with 53BP1 is dependent on phosphorylation, we performed Western blot analysis of Flag immunoprecipitates from lysates of irradiated $Trp53bp1^{-/-}$ B cells infected with retroviruses encoding $53BP1^{DB}$ or $53BP1^{DB28A}$. Whereas Dynll1, a phospho-independent 53BP1 interactor (SILAC ratio: 0.55) (fig. S1D), coimmunoprecipitated with $53BP1^{DB}$ and $53BP1^{DB28A}$ to a similar extent (Fig. 2A), only $53BP1^{DB}$ coimmunoprecipitated with Rif1. We conclude that the interaction between 53BP1 and Rif1 is dependent on phosphorylation of 53BP1.

Ataxia-telangiectasia mutated phosphorylates 53BP1 in response to DSBs (1, 3). To determine whether ATM induces DNA damage–dependent association between Rif1 and 53BP1, we compared irradiated and nonirradiated B cells in coimmunoprecipitation experiments. Although we detected small amounts of Rif1 in $53BP1^{DB}$ immunoprecipitates from unirradiated cells, this was increased by a factor of >3 after irradiation, and the increase was abrogated by treatment with the ATM inhibitor KU55933 (Fig. 2B). We conclude that Rif1 preferentially interacts with phosphorylated 53BP1 in a DNA damage- and ATM-dependent manner.

Rif1 is recruited to DNA damage foci by 53BP1 (15). To determine whether 53BP1 phosphorylation is required for Rif1 focus formation, we tested Rif1 foci in irradiated $Trp53bp1^{-/-}$ immortalized mouse embryonic fibroblasts (iMEFs), which were stably transduced with either $53BP1^{DB}$ or $53BP1^{DB28A}$. Rif1 foci were readily detected and colocalized with $53BP1^{DB}$ (Fig. 2C). In contrast, although $53BP1^{DB28A}$ formed normal-appearing foci, Rif1 foci were rare and did not colocalize with 53BP1 (Fig. 2C). Furthermore, Rif1 recruitment to ionizing radiation–induced foci (IRIF) and colocalization with 53BP1 were abrogated in ATM-deficient but not DNA-PKcs–deficient iMEFs (fig. S3) (15). We conclude that Rif1 recruitment to DNA damage response foci is dependent on ATM-mediated 53BP1 phosphorylation.

The phosphorylation of 53BP1 is essential for CSR (4). To examine the role of Rif1 in joining DSBs during CSR, we conditionally ablated Rif1 in B cells using CD19^Cre, which is expressed specifically in B cells ($Rif1^{F/F}Cd19^{Cre/+}$ mice) (fig. S4, A to C). To induce CSR, B cells were activated with lipopolysaccharide (LPS) and interleukin-4 (IL-4) in vitro, and switching to immunoglobulin G1 (IgG1) or IgG3 was mea-

sured by flow cytometry. CSR to IgG1 and IgG3 was markedly reduced in $Rif1^{F/F}Cd19^{Cre/+}$ B cells, but less so than in $Trp53bp1^{-/-}$ controls (Fig. 3, A and B, and fig. S5). Switch junctions from $Rif1^{F/F}Cd19^{Cre/+}$ B cells were comparable to those from $Trp53bp1^{-/-}$ and wild-type controls (fig. S6) (7), which indicates that, similar to 53BP1 deficiency, absence of Rif1 does not alter the nature of productive CSR joining events.
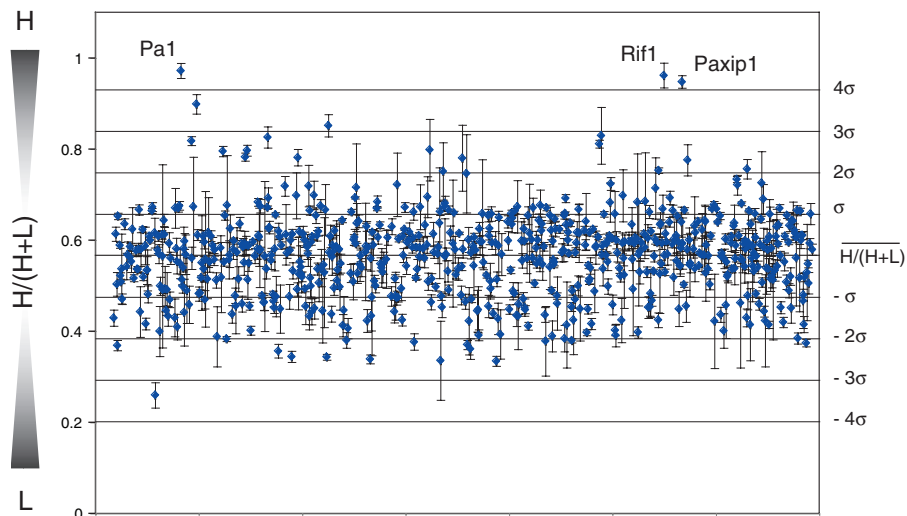

Fig. 1. Identification of phospho-dependent 53BP1 interactors. The graph shows the $H/(H + L)$ ratio distribution of proteins identified by SILAC. Error bars represent the SD of the $H/(H + L)$ mean value for all of the peptides identified for each individual protein (only proteins with at least four peptides were included). $\overline{H/(H + L)}$ and σ are the mean (0.57) and SD (0.09) of the distribution, respectively.
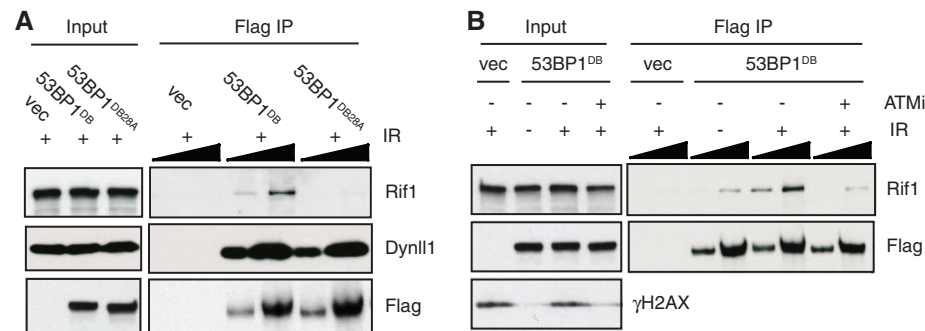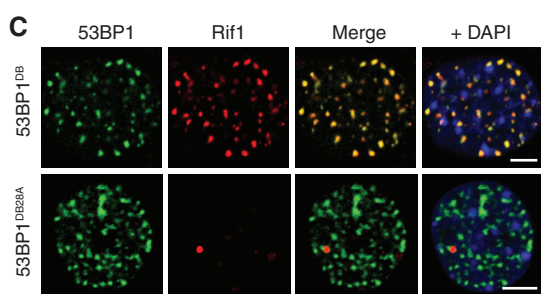

Fig. 2. Rif1 interaction with 53BP1 is dependent on phosphorylation, DNA damage, and ATM. (**A**) Western blot analysis of anti-Flag immunoprecipitates (IP) from irradiated (IR) $Trp53bp1^{-/-}$ B lymphocytes infected with empty vector (vec), $53BP1^{DB}$, or $53BP1^{DB28A}$ virus. Triangles indicate threefold dilution. Data are representative of two independent experiments. (**B**) Western blot analysis of anti-Flag immunoprecipitates from $Trp53bp1^{-/-}$ B cells infected with empty vector or $53BP1^{DB}$. Cells were either left untreated or irradiated [50 gray (Gy), 45-min recovery] in the presence or absence of the ATM kinase inhibitor KU55933 (ATMi). Triangles indicate threefold dilution. Data are representative of two independent experiments. (**C**) Immunofluorescent staining for 53BP1 (Flag) and Rif1 in irradiated $Trp53bp1^{-/-}$ iMEFs reconstituted with $53BP1^{DB}$ or $53BP1^{DB28A}$ retroviruses (4). Magnification, 100×; scale bars, 5 μm. Data are representative of two independent experiments. DAPI, 4′,6-diamidino-2-phenylindole.
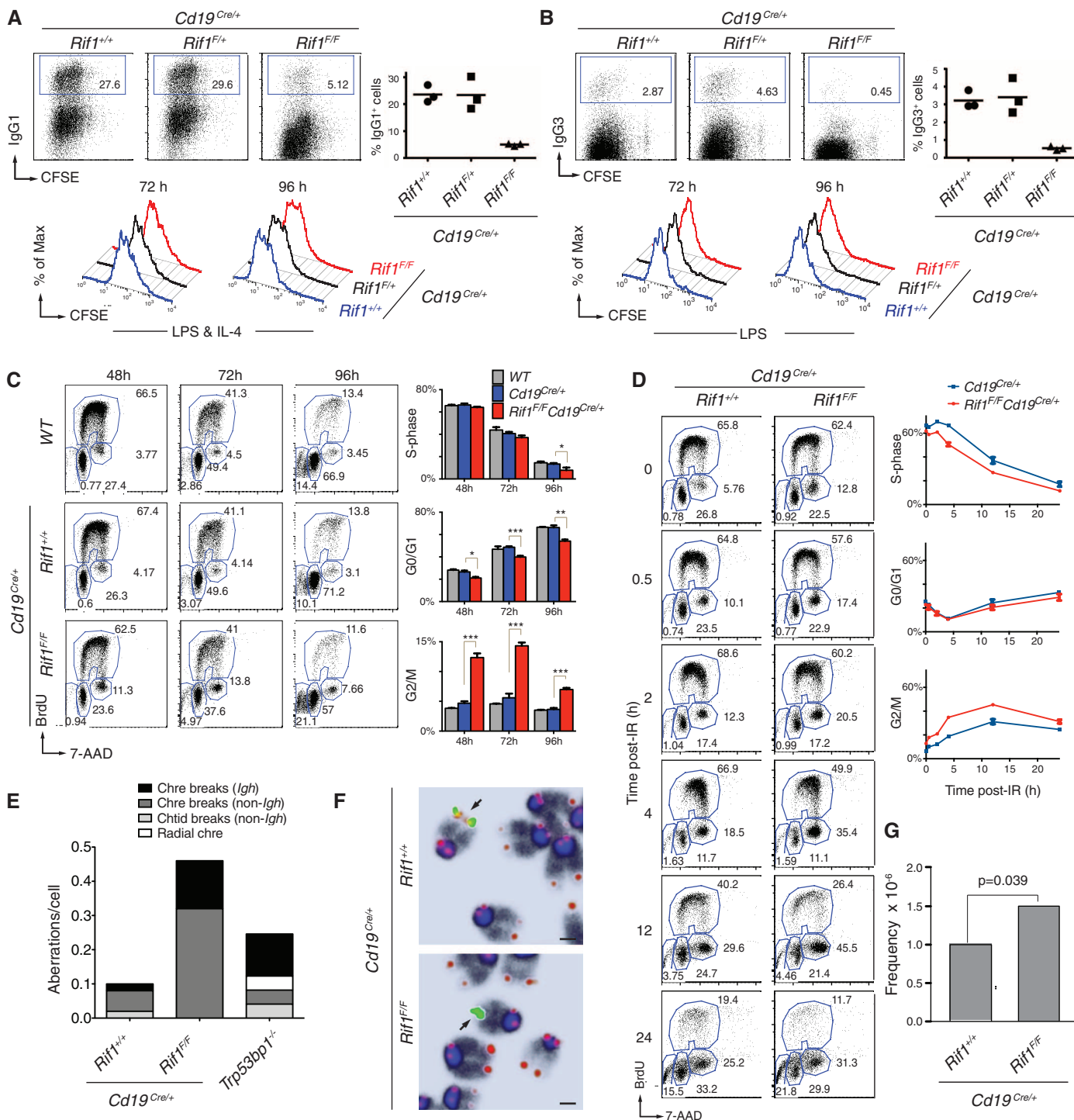
Fig. 3. Rif1 deficiency impairs CSR and causes *Igh* and genome instability in primary B cells. (**A**) (Left) CSR to IgG1 96 hours after stimulation of B lymphocytes with LPS and IL-4. (Right) Summary dot plot for three independent experiments (*n* = three mice per genotype). Mean values are: 23.6% for *Cd19^Cre/+^*, 23.4% for *Rif1^F/+^Cd19^Cre/+^*, and 5.0% for *Rif1^F/F^Cd19^Cre/+^* (*P* < 0.008 with the paired Student's *t* test). (Bottom) B cell proliferation by carboxyfluorescein succinimidyl ester (CFSE) dilution. Data are representative of three independent experiments. (**B**) Same as in (A) but for CSR to IgG3 after stimulation with LPS alone. Mean values are: 3.2% for *Cd19^Cre/+^*, 3.4% for *Rif1^F/+^Cd19^Cre/+^*, and 0.5% for *Rif1^F/F^Cd19^Cre/+^* (*P* < 0.008). (**C**) (Left) Cell cycle analysis of primary B cells after stimulation with LPS and IL-4. BrdU, 5-bromo-2'-deoxyuridine; 7-AAD, 7-amino-actinomycin D. (Right) Summary histograms for S, G_0/G_1, and G_2/M phase cells from two independent experiments (*n* = four mice per genotype). Error bars indicate SEM.

* 0.01 < *P* < 0.05, ** 0.001 < *P* < 0.01, *** *P* < 0.001. WT, wild type. (**D**) (Left) Cell cycle analysis of LPS- and IL-4–stimulated splenocytes at the indicated times after irradiation (6 Gy). (Right) Summary graphs for S, G_0/G_1, and G_2/M phase cells from two independent experiments (*n* = three mice per genotype). Error bars indicate SD. (**E**) Analysis of genomic instability in metaphases from B cell cultures. Chtid, chromatid; Chre, chromosome. Data are representative of two independent experiments (*n* = 50 metaphases analyzed per genotype per experiment). (**F**) Examples of *Igh*-associated aberrations in *Rif1^F/F^Cd19^Cre/+^* B cells. Chromosomes were hybridized with an *Igh* Cα probe (green; centromeric of Cγ1) and a telomere sequence-specific probe (red) and were counterstained with DAPI (dark blue/black). Arrows indicate *Igh* Cα/telomeric signal on chromosome 12. Magnification, 63×; scale bars, 1 μm. (**G**) Frequency of *c-myc/Igh* translocations in activated B cells. The graph shows combined results from three mice per genotype.

A similar CSR defect was also obtained by conditionally deleting Rif1 with 4-hydroxy-tamoxifen (4HT) in $Rif1^{F/F}ROSA26^{Cre-ERT2/+}$ B cells (fig. S7). Finally, short hairpin RNA–mediated partial down-regulation of CtBP-interacting protein (CtIP), which interacts with Rif1 (fig. S8C) and has been implicated in processing of DNA ends (21, 22), resulted in a very small but reproducible increase in CSR (fig. S8, A and B). Thus, Rif1 is essential for normal CSR, and CtIP may not be the only factor that contributes to end processing in Rif1-deficient B cells.

Class switch recombination requires cell division, activation-induced cytidine deaminase (AID) expression, and Igh germline transcription (23). There are conflicting reports that Rif1 is required for proliferation in MEFs, but not in DT40 B cells (17, 18). We found that cell division profiles of $Rif1^{F/F}Cd19^{Cre/+}$ and 4HT-treated $Rif1^{F/F}ROSA26^{Cre-ERT2/+}$ B cells were indistinguishable from controls (Fig. 3, A and B; and fig. S7, A, C, E, and G), indicating that Rif1 is dispensable for B cell proliferation in vitro. Finally, AID mRNA and protein expression and Igh germ-

line transcription were not affected by Rif1 deletion (fig. S4, B and D).

We next examined the role of Rif1 in cell cycle progression in primary B cells. We found no major differences in the percentage of cells in G_0/G_1 and S phases (Fig. 3C). However, the number of cells in G_2/M phase was increased approximately twofold in the absence of Rif1 (2.64-, 2.56-, and 1.91-fold at 48, 72, and 96 hours, respectively) (Fig. 3C). We obtained similar results with the use of $Rif1^{F/F}ROSA26^{Cre-ERT2/+}$ B cells treated with 4HT (fig. S7, H and I).
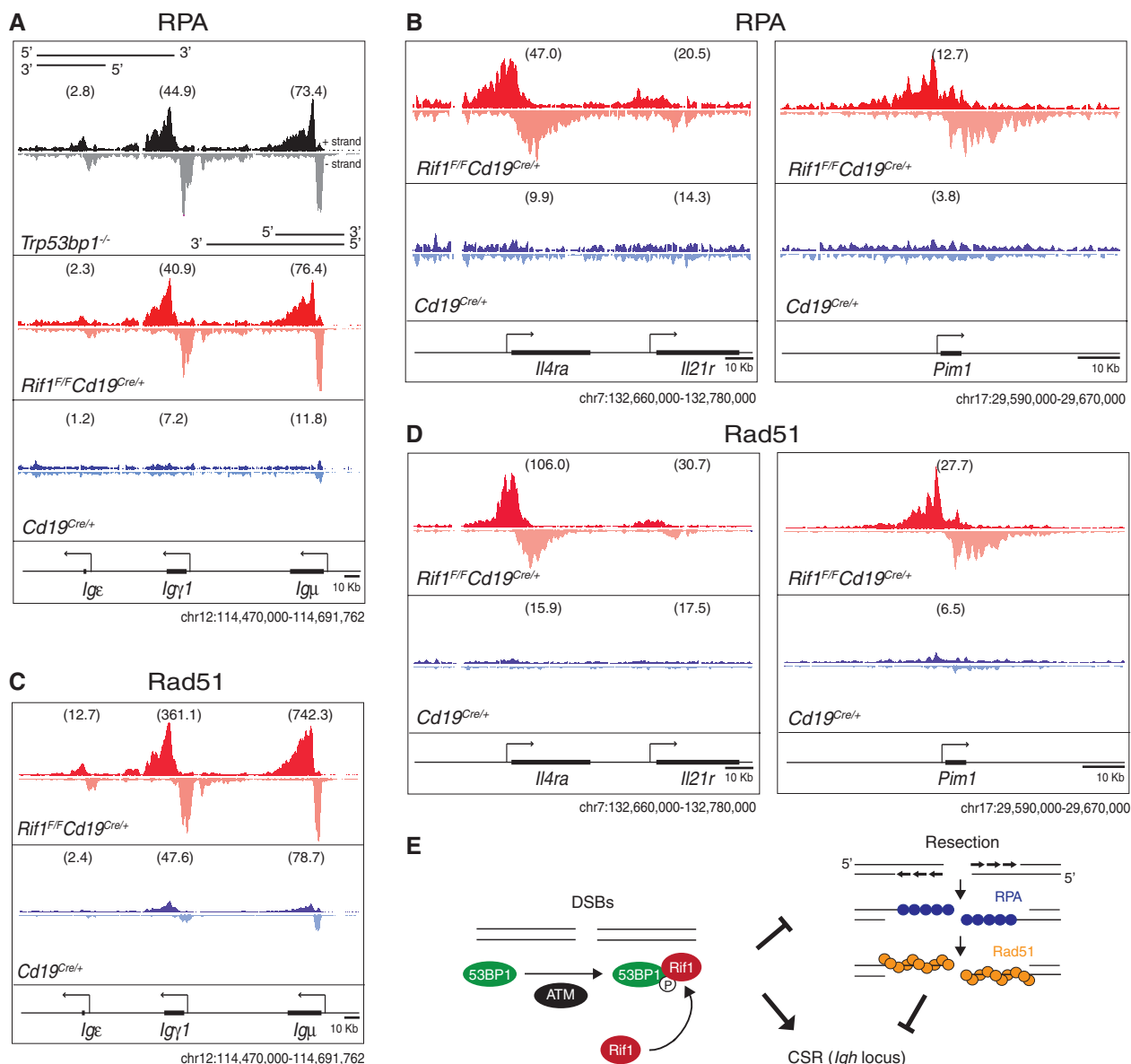

Fig. 4. Rif1 prevents resection of DNA ends at sites of AID-induced DNA damage. (**A** to **D**) RPA and Rad51 occupancy at the Igh locus (A and C) and at non-Igh AID targets genes (B and D) in B cells activated to undergo class switching. ChIP-seq libraries were resolved into upper (+) and lower (-) DNA strands to show RPA and Rad51 association with sense and antisense strands. Within a specified genomic window, graphs have the same scale and show tag density. Deep-sequencing samples were normalized per library size, and tags per million values were calculated for each genic region, as indicated in the supplementary materials and methods and shown in parenthesis. Data are representative of two independent experiments for RPA ChIP-seq and one for Rad51. (**E**) Model of Rif1 recruitment and DNA-end protection at DSBs. DNA damage activates ATM, which phosphorylates many targets, including 53BP1. This event recruits Rif1 to 53BP1 at the DSB, where it inhibits DNA resection. The extensive resection in the absence of Rif1 impairs CSR at the Igh locus. P, phosphate.

Furthermore, irradiation increases the accumulation of $Rif1^{F/F}Cd19^{Cre/+}$ B cells in G2/M phase (Fig. 3D). In addition, $Trp53bp1^{-/-}$ iMEFs expressing 53BP1^{DB28A}, which did not recruit Rif1 to IRIF (Fig. 2C), exhibited delayed progression through S phase following DNA damage with accumulation of cells in G$_2$ phase after irradiation (fig. S9).

Accumulation of cells in G$_2$/M phase may reflect the persistence of unrepaired DNA damage in a fraction of Rif1-deficient cells. To investigate this possibility, we analyzed metaphase spreads from B cells dividing in response to LPS and IL-4 in vitro. These cells express AID, which produces DSBs in *Igh* and, less frequently at off-target sites throughout the genome, in the G$_1$ phase of the cell cycle (*24–26*). Chromosomal aberrations were increased in $Rif1^{F/F}Cd19^{Cre/+}$ B cells compared to controls (Fig. 3E), with many localized to the *Igh* locus (Fig. 3E). Consistent with the observation that *Igh* is targeted by AID in the G$_1$ phase of the cell cycle, all of the *Igh* breaks were chromosome breaks (Fig. 3, E and F). Interestingly, the frequency of *c-myc/Igh* translocations is moderately increased in $Rif1^{F/F}Cd19^{Cre/+}$ B cells; however, the breakpoint distribution was similar to the $Cd19^{Cre/+}$ control (1.5×10^{-6} versus 1.0×10^{-6} in the control; $P = 0.039$) (Fig. 3G and fig. S10). We conclude that in the absence of Rif1, DSBs fail to be resolved efficiently in the G$_1$, S, or G$_2$ phases, which leads to increased levels of genomic instability, including chromosome breaks at *Igh* and translocations in dividing B cells.

In the absence of 53BP1, DSBs produced by AID at the *Igh* locus accumulate the single-stranded DNA-binding replication protein A complex (RPA) as a result of increased DNA-end resection (*24*). To determine if Rif1 is required for DNA-end protection by 53BP1, we performed RPA–chromatin immunoprecipitation followed by massive parallel sequencing (ChIP-seq) experiments on $Rif1^{F/F}Cd19^{Cre/+}$ and control B cells. Ablation of Rif1 was indistinguishable from the loss of 53BP1 in that in its absence, RPA decorates the *Igh* locus asymmetrically, in a manner consistent with 5'-3' resection (Fig. 4A) (*27*). In addition, absence of Rif1 also results in RPA accumulation at non-*Igh* genes, such as *Il4ra* and *Pim1*, that are damaged by AID in G$_1$ phase (Fig. 4B) (*24*, *25*). Rad51 is the recombinase that mediates repair of DSBs by homologous recombination in S/G$_2$/M phase (*22*). To confirm that Rif1 prevents resection that takes place in S phase, we monitored Rad51 accumulation in activated B cells by ChIP-seq. Loss of Rif1 was

indistinguishable from the loss of 53BP1 (*27*), in that it led to asymmetric Rad51 accumulation at sites of AID-inflicted DNA damage (Fig. 4, C and D). We conclude that in the absence of Rif1, AID-induced DSBs incurred in G$_1$ phase persist and undergo extensive 5'-3' DNA-end resection in S/G$_2$/M phase, as measured by RPA and Rad51 accumulation.

A role for Rif1 in maintenance of genome stability and protection of DNA ends against resection is consistent with its phosphorylation-dependent recruitment to the N-terminal domain of 53BP1 (*4*). 53BP1 facilitates DNA repair and prevents DNA-end resection during CSR. In the absence of 53BP1, AID-induced DSBs are resolved inefficiently in G$_1$ phase, leading to chromosome breaks, *Igh* instability, and resolution by alternative NHEJ or homologous recombination instead of classical NHEJ (*4*, *8*, *27*). Our experiments show that in the absence of Rif1, 53BP1 is insufficient to promote genomic stability or mediate efficient *Igh* repair, DNA-end protection, or CSR. Thus, these 53BP1 activities require Rif1 recruitment to the phosphorylated N terminus of 53BP1. Rif1 is likely to have additional functions beyond 53BP1, CSR, and DNA-end protection because although $Trp53bp1^{-/-}$ mice are viable, Rif1 deletion is lethal (*17*). Indeed, Rif1 is believed to play a role in the repair of S-phase DNA damage (*17*, *18*), as well as in the regulation of replication timing (*19*, *20*, *28*). Analogously, additional CSR factor(s) may exist downstream of 53BP1, as class switching in Rif1-deficienct B cells is significantly higher than in $Trp53bp1^{-/-}$.

In summary, our data are consistent with a model in which ATM-mediated phosphorylation of 53BP1 recruits Rif1 to sites of DNA damage, where it facilitates DNA repair in part by protecting DNA ends from resection (Fig. 4E). In the absence of Rif1, DNA breaks incurred in G$_1$ phase fail to be repaired by NHEJ and undergo extensive 5'-3' end resection, resulting in the accumulation of chromosome breaks and genome instability.

References and Notes

1. M. M. Adams, P. B. Carpenter, *Cell Div.* **1**, 19 (2006).
2. J. Lukas, C. Lukas, J. Bartek, *Nat. Cell Biol.* **13**, 1161 (2011).
3. A. T. Noon, A. A. Goodarzi, *DNA Repair* **10**, 1071 (2011).
4. A. Bothmer et al., *Mol. Cell* **42**, 319 (2011).
5. S. Difilippantonio et al., *Nature* **456**, 529 (2008).
6. N. Dimitrova, Y. C. Chen, D. L. Spector, T. de Lange, *Nature* **456**, 524 (2008).
7. B. Reina-San-Martin, J. Chen, A. Nussenzweig, M. C. Nussenzweig, *Eur. J. Immunol.* **37**, 235 (2007).
8. A. Bothmer et al., *J. Exp. Med.* **207**, 855 (2010).
9. J. P. Manis et al., *Nat. Immunol.* **5**, 481 (2004).
10. I. M. Ward et al., *J. Cell Biol.* **165**, 459 (2004).
11. Materials and methods are available as supplementary materials on *Science* Online.
12. I. A. Manke, D. M. Lowery, A. Nguyen, M. B. Yaffe, *Science* **302**, 636 (2003).
13. C. F. Hardy, L. Sussel, D. Shore, *Genes Dev.* **6**, 801 (1992).
14. S. Kumar et al., *Cell Cycle* **11**, 1183 (2012).
15. J. Silverman, H. Takai, S. B. Buonomo, F. Eisenhaber, T. de Lange, *Genes Dev.* **18**, 2108 (2004).
16. L. Xu, E. H. Blackburn, *J. Cell Biol.* **167**, 819 (2004).
17. S. B. Buonomo, Y. Wu, D. Ferguson, T. de Lange, *J. Cell Biol.* **187**, 385 (2009).
18. D. Xu et al., *EMBO J.* **29**, 3140 (2010).
19. D. Cornacchia et al., *EMBO J.* **31**, 3678 (2012).
20. S. Yamazaki et al., *EMBO J.* **31**, 3667 (2012).
21. A. A. Sartori et al., *Nature* **450**, 509 (2007).
22. L. S. Symington, J. Gautier, *Annu. Rev. Genet.* **45**, 247 (2011).
23. R. Pavri, M. C. Nussenzweig, *Adv. Immunol.* **110**, 1 (2011).
24. O. Hakim et al., *Nature* **484**, 69 (2012).
25. S. Petersen et al., *Nature* **414**, 660 (2001).
26. A. Yamane et al., *Nat. Immunol.* **12**, 62 (2011).
27. A. Yamane et al., *Cell Rep.* 10.1016/j.celrep.2012.12.006 (2013).
28. M. Hayano et al., *Genes Dev.* **26**, 137 (2012).